

AD-A041 831

NORTHWESTERN UNIV EVANSTON ILL DEPT OF MATERIALS SCIENCE  
A PORTABLE RESIDUAL STRESS ANALYZER. (U)

F/G 20/11

JUL 77 M R JAMES, J B COHEN

N00014-75-C-0580

UNCLASSIFIED

TR-19

NL

| OF |  
ADA041831



END

DATE  
FILMED

8 - 77

AD A041831

NORTHWESTERN UNIVERSITY

DEPARTMENT OF MATERIALS SCIENCE

Technical Report No. 19  
July 12, 1977

Office of Naval Research  
Contract N00014-75-C-0580  
NR 031-733

A PORTABLE RESIDUAL STRESS ANALYZER \*

by

M. R. James and J. B. Cohen

11 12 Jul 77

D D C  
REPAIRED  
JUL 21 1977  
C

Distribution of this Document  
is Unlimited

12 36p. 14 TR-19

Reproduction in whole or  
in part is permitted for  
any purpose of the United  
States Government.



EVANSTON, ILLINOIS

1473  
260 810

AD No.  
DDC FILE COPY

# A PORTABLE RESIDUAL STRESS ANALYZER

M. R. James and J. B. Cohen

Northwestern University

Evanston, Illinois 60201

## ABSTRACT

A portable device for stress measurements based on a position sensitive detector and using a miniature air-cooled X-ray tube was built to demonstrate the potential of such a system. The measuring apparatus, weighing 11 kg, could be held by one person with the electronics housed in a separate cabinet. A variety of steel samples, having from 0 to -700 MPa were tested by comparing measurements made on a diffractometer to those made with the portable device. The device proved to be accurate and accomplished the entire measurement using two <sup>+1-</sup> tilts to a statistical error of less than  $\pm 40$  MPa in under 20 seconds on all samples. (In some cases in 4 seconds.) The portability of the apparatus and rapid measurement time suggest applications for the X-ray stress measurement never possible before, such as on-sight inspection during fabrication or in-field measurements.

PSI

APPROVAL DATE	
1/15	WHITE SECTION
1/15	BUFF SECTION
UNAUTHORIZED	
JUSTIFICATION	
DISTRIBUTION/AVAILABILITY CODES	
DISL	AVAIL. AND/OR SPECIAL
	

## CHAPTER 7\*

## 7.1 INTRODUCTION

The design of any mechanical system is based around those features it is desired to optimize. In the case of residual stress analysis by X-ray diffraction methods, an accurate, rapid and portable device is needed if the technique is to be more widely used in industry. (101) Dedicated apparatus for measuring the surface residual stress have been commercially available, but are limited in flexibility and precision. Commercially available apparatus is reviewed in Sec. 7.2 and the use of an energy dispersive X-ray system for residual stress analysis is discussed. These instruments are not portable and the time of analysis are not fast enough to be considered for use on production lines or for quality control.

A design based on a position sensitive detector is described. In order to obtain the best design, a theoretical consideration is made of the relationship between the time of analysis and the total accuracy by taking into account the factors that influence each quantity. The time of analysis is strictly determined by counting statistics while the accuracy is related both to the statistics and to systematic errors in the measurement. The major design factor involving both of these quantities is the sample to detector distance, R; the counting precision improves at smaller R while the systematic errors increase.

A prototype of the portable apparatus was built and shown to be capable of measuring the residual stress to a total accuracy better than  $\pm 40$  MPa in 4-20 sec. on all types of steel samples. The instrument uses

---

\* Chs. 1-3 constitute TR No. 14, Ch. 4 is TR No. 16, Ch. 5 is TR No. 15, and Ch. 6 is TR No. 17.

the two tilt method, stationary-slit geometry and incorporates a position sensitive detector with an air-cooled X-ray tube. The actual hand held goniometer weighs only 11 kg and a reduction to 7 kg is outlined. There are two modest cabinets the size of a potentiometer, one for the X-ray generator and one for the circuitry for data analysis.

## 7.2 PRIOR INSTRUMENTATION

Development of dedicated instrumentation in the field of X-ray stress analysis have usually been based on modifications and innovations associated with or built around a diffractometer. The Fastress<sup>(98)</sup> unit utilizes two X-ray tubes and two pair of detectors to locate the peak, one pair each at  $\psi=0^\circ$  and at  $\psi=45^\circ$ . Both peak positions are found by matching the intensity in each detector with its mate, which is positioned on the other side of the profile. The midpoint between the two detectors is used for the peak location. Both pairs of detectors are calibrated in terms of angular position so the peak shift can be electronically determined, assuming the diffraction profile is symmetric and the detector efficiencies are matched. Reproducibility is about  $\pm 20$  MPa in a 3 minute test on hardened steel samples. The device is semi-portable in that the measuring head (incorporating the X-ray tube, detectors and 2 $\theta$  motion), electronics and power supply may be rolled on a cart in the laboratory.

Another dedicated unit, the Shimadzu X-Ray Diffraction stress analyzer,<sup>(99)</sup> uses normal scanning of the profile to locate the peak. Two peaks at different  $\psi$  inclinations may be scanned at once using two X-ray tubes and two detectors mounted on one goniometer head. The device is capable of the  $\sin^2\psi$  analysis but uses a separate calculator to determine the stress.

Simultaneous with this study on the position sensitive detector, Campagnie General de Radiologie, Paris, France, manufactured a new instrument for the measurement of residual stress.<sup>(102)</sup> Their device incorporates two PSD's as shown in Fig. 7.1. The detectors are proportional counters using the rise time method of position determination similar to that used in this study. The adjacent ends B and C of the detectors are conductively connected together and the outer ends A and D are connected to two rise time measuring circuits. Figure 7.2 schematically depicts the output of the device stored on a MCA. In Fig. 7.2a the output for a stress free specimen is shown. In Fig. 7.2b a sample having a stress will give rise to a shift in the position of each profile. The change is measured relative to an unstressed specimen and calibration must be carried out by analyzing a second specimen subjected to a known amount of stress. While this procedure is accurate it is time consuming, so the inventor suggests that the single exposure method can also be used.

The stress component is measured from a single inclination by determining the Bragg angle at two positions on the diffraction ring. If the incident X-ray beam is directed toward the specimen surface at a fixed angle  $\theta$  from the surface normal, as seen in Fig. 7.1, the two Bragg angles will be shifted because the interplanar spacings of the diffracting crystallites are different due to the residual stress. The diffraction angles can be related to the stress.

The stress constant for the single exposure method is larger than the two tilt method. For example, for the Fe 211 peak the stress constant for the two tilt technique, using a tilt of  $60^\circ$  is one half that for the single exposure method with  $\theta=35^\circ$ .

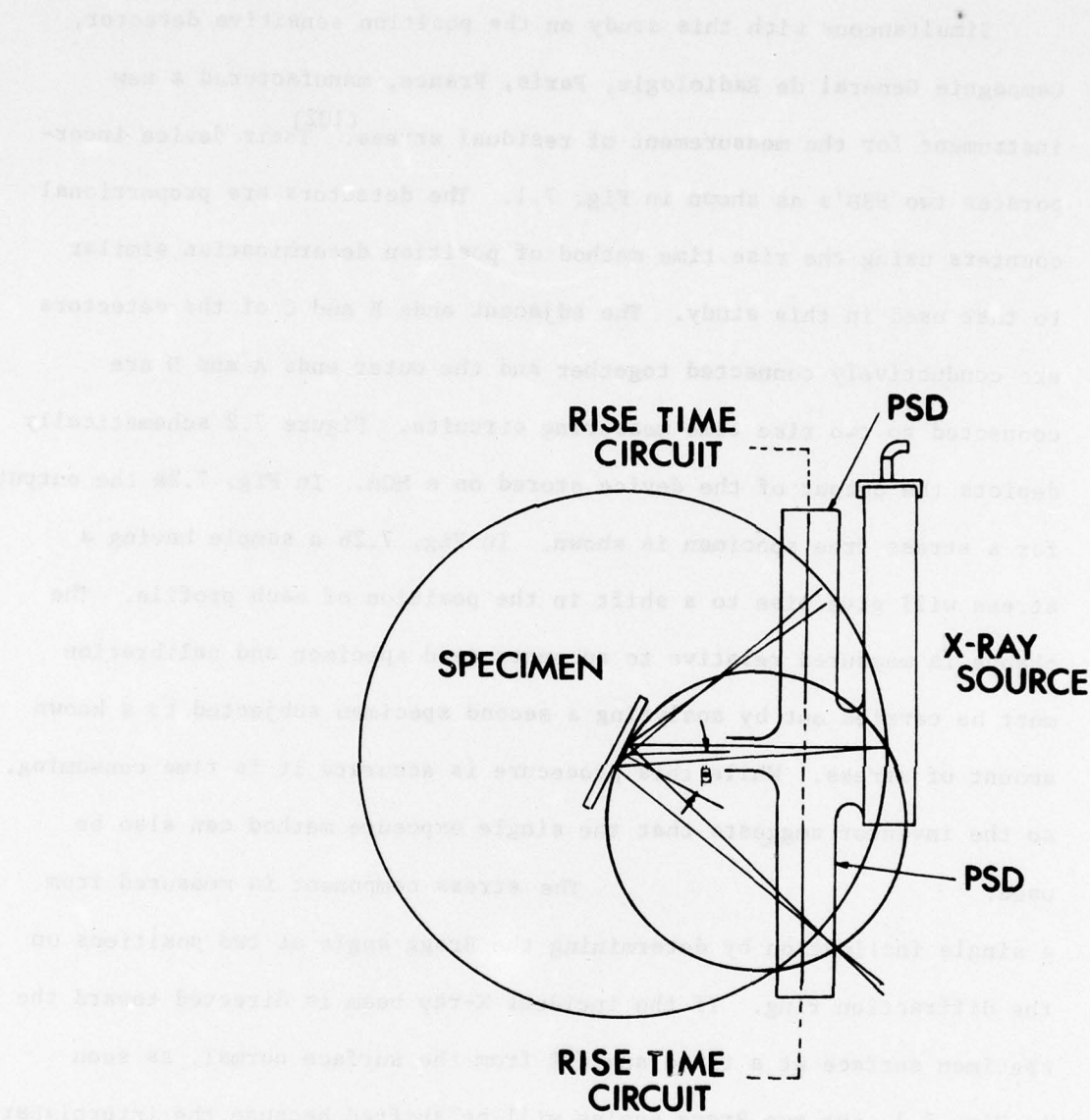


**FIGURE 7.1** Embodiment of apparatus utilizing the single exposure technique.  
From reference 102.

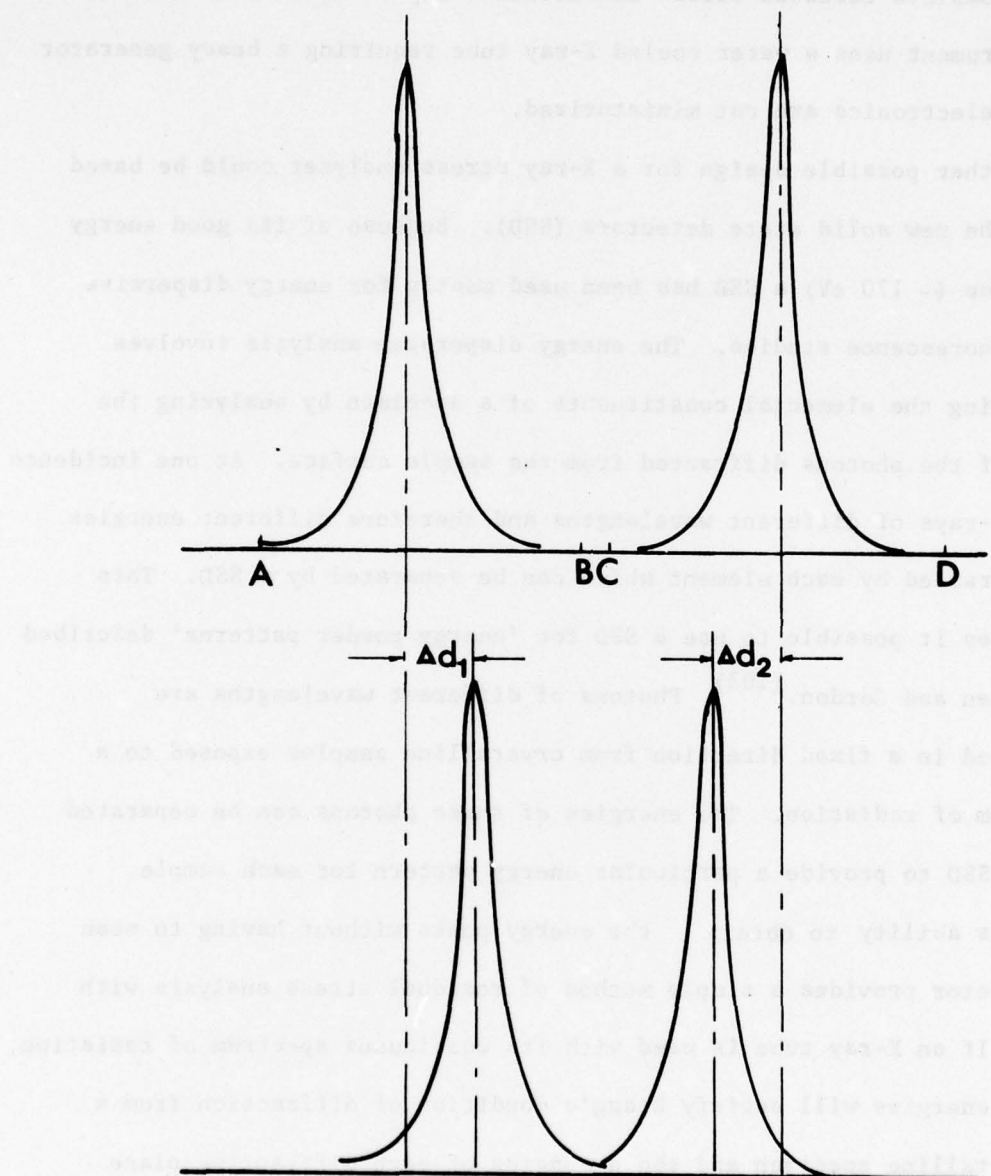


FIGURE 7.2 Illustration of the operation of the single exposure apparatus.  
 a) Stress-free sample  
 b) Sample with compressive stress.

This means that the counting errors become more important for the single exposure method requiring longer data collection times. The manufacturer claims complete residual stress measurements may be made in 15 minutes. The instrument uses a water cooled X-ray tube requiring a heavy generator and the electronics are not miniaturized.

Another possible design for a X-ray stress analyzer could be based around the new solid state detectors (SSD). Because of its good energy resolution ( $\sim 170$  eV) a SSD has been used mostly for energy dispersive X-ray fluorescence studies. The energy dispersive analysis involves determining the elemental constituents of a specimen by analyzing the energy of the photons diffracted from the sample surface. At one incidence angle, X-rays of different wavelengths and therefore different energies are diffracted by each element which can be separated by a SSD. This also makes it possible to use a SSD for 'energy powder patterns' described by Giessen and Gordon.<sup>(103)</sup> Photons of different wavelengths are diffracted in a fixed direction from crystalline samples exposed to a continuum of radiation. The energies of these photons can be separated using a SSD to provide a particular energy pattern for each sample.

This ability to obtain the energy peaks without having to scan the detector provides a simple method of residual stress analysis with a SSD. If an X-ray tube is used with its continuous spectrum of radiation, certain energies will satisfy Bragg's condition of diffraction from a polycrystalline specimen and the d spacing of each diffracting plane can be determined from the peaks in energy.

Rewriting Bragg's law in terms of energy:

$$\lambda = 2d \sin \theta$$

and

$$U = hc/\lambda$$

$$\text{so that } U d \sin \theta = hc/\lambda = 6195(\text{eV}) (\text{\AA}) \quad (7.1)$$

where  $U$  is in eV,  $d$  in  $\text{\AA}$  and  $h$  and  $c$  are Plank's constant and the speed of light respectively. By measuring the peaks in energy at  $\psi=0^\circ$  and at an inclination,  $\psi=\psi^\circ$ , the energy shift can be determined. Residual stress changes the  $d$  spacing of the crystallites at  $\psi=0$  and at  $\psi=\psi^\circ$  which results in photons of different energies being diffracted at each tilt. To determine a typical magnitude of the energy shift, the stress can be determined by the two tilt method as follows:

$$\sigma_\psi = \left( \frac{E}{1+\nu} \right) \frac{1}{\sin^2 \psi} \frac{d_{\psi, \psi} - d_0}{d_0} \quad (7.2)$$

Substituting in Eq. 7.1

$$\sigma_\psi = \left( \frac{E}{1+\nu} \right) \left( \frac{1}{\sin^2 \psi} \right) \left( \frac{U_0 - U_{\psi, \psi}}{U_0} \right) \quad (7.3)$$

Using elastic constants for steel of  $E = 207 \text{ GPa}$  ( $30.02 \times 10^6 \text{ psi}$ ) and  $\nu = .33$  and a tilt of  $\psi=45^\circ$  the resultant energy shift for a stress of  $-70 \text{ MPa}$  ( $-10152 \text{ psi}$ ) is  $(U_0 - U_{\psi, \psi})/U_{\psi, \psi} = 2.22 \times 10^{-4}$ . For X-rays in the range of 6 keV this implies an energy shift of 1.3 eV, a very small shift to determine with a SSD having a resolution at half width of a

5.94 keV X-ray peak of 170 eV. If it is assumed the peak shift can be determined to 5 eV, still a liberal estimate,  $U_0$  must be near 25 keV. Such energies can be obtained using the white radiation of an X-ray tube. It is convenient that the diffraction angle need not be known thereby eliminating experimental errors.\* However, such a technique must suffer drastically in intensity. Cole<sup>(104)</sup> has derived an expression for the total diffracted power from a flat powder sample as:

$$P' = P(\lambda_{hkl}) \left( \frac{e^4}{m^2 c^4} \right) \frac{m}{16\pi R v_a} \frac{\lambda^4 F^2}{2\mu} \left( \frac{1+\cos^2 2\theta}{2\sin^3 \theta} \right) \quad (7.4)$$

where  $P'$  is the power per unit length of the diffracted cone,  $m$ , the multiplicity of the powder line,  $R$ , the sample-to-detector distance, and  $\lambda$  and  $\mu$  are characteristic of the diffracted photon. Since if there are no absorption edges,  $\mu$  depends on  $\lambda^3$ ,<sup>(105)</sup> the diffracted power falls off roughly as  $\lambda$ . Also in the structure factor,  $F$ , the term involving the Debye-Waller factor ( $e^{-\theta \sin^2 \theta / \lambda^2}$ ) falls off as  $e^{-1/\lambda^2}$ . For energies of 25 keV ( $\lambda \sim .5 \text{ \AA}$ ) the total diffracted power will be very small due to the short wavelength. In summary, while the use of a SSD for stress measurements using the energy dispersive mode is possible, the diffracted intensity will be quite low resulting in long counting times.

The best system would seem to be based on a PSD, but avoiding the pitfalls of the single exposure method.

---

\*The  $\psi$ -axis missetting is still important because Eq. 7.3 is based on fixed  $\sin \theta$ .

7.3 CALCULATION OF OPTIMUM PARAMETERS FOR THE DESIGN OF A PORTABLE RESIDUAL STRESS ANALYZING SYSTEM

The precision of the measurement of stress is dependent on the counting statistical accuracy and the systematic experimental errors. The statistical accuracy, being a function of the total number of counts, is dependent on the intensity of the detected photons and the time of data collection. The systematic errors include the resolution and calibration of the detector system and instrumental errors such as  $\psi$ -axis missetting and specimen positioning. The relationship between each factor and the sample-to-detector distance has been considered in order to optimize the distance for a minimum time of analysis.

7.3.1 Relation Between Statistical Accuracy and the Sample-to-Detector Distance

The counting statistical error in stress is

$$\sigma^2(2\theta_p) = \frac{1}{C} \sum_j \left( \frac{\partial 2\theta_p}{\partial I_j} \right)^2 I_j^2 \quad (7.5)$$

where  $C$  is the fixed counts

accumulated at each observation point,  $j$ . The summed term depends on the intensity, step size between data points and breadth of the peak. For each individual profile, these quantities are independent of the preset count allowing Eq. 7.5 to be rewritten as

$$\sigma^2(2\theta_p) = Q_1/C \quad (7.6)$$

where  $Q_1$  is a constant representing the summed term in Eq. 7.5. This quantity can be determined from an initial step scan across the diffraction profile.

The fixed counts,  $C$ , can be written in terms of the diffracted power,  $I_j$ , in cps and the time,  $t_j$ , of data accumulation at each observation point  $j$ :

$$C = I_j \cdot t_j \quad (7.7)$$

Then:

$$\sigma^2(2\theta p) = Q_1 / (I_j \cdot t_j) \propto 1/I \cdot T \quad (7.8)$$

where  $I$  is the average power and  $T$  is the total time of data accumulation.

The power is a function of  $R$ , the sample to detector distance due to the absorption in air and the  $1/R$  dependence of the power itself at each  $2\theta$  position. The path length in air is  $2R$  so the absorption factor is given by

$$\frac{I}{I_0} = \exp[-(\mu/\rho) \cdot \rho \cdot 2R] \quad (7.9)$$

where

$$\mu/\rho = \sum_i (\mu/\rho)_i w_i$$

and  $w_i$  is the weight fraction of the  $i^{\text{th}}$  element. Assuming the density of air to be 78%  $N_2$ , 21%  $O_2$  and 1%  $Ar$  and using values for the absorption coefficients for  $Cr_{K\alpha}$  radiation from reference 105, the effect of air absorption for  $Cr_{K\alpha}$  radiation is:

$$I \propto e^{-0.07R} \quad (7.10)$$

where R is in cm.

For a powder sample the intensity from each atom is proportional to  $R^{-2}$  but the power at each angle is proportional to this times  $R^2$ . In addition, the power per unit length of the powder diffraction cone is equal to the total power divided by  $2\pi R \sin 2\theta$ .<sup>(107)</sup> In sum the power at each angle in a peak in a powder pattern is proportional to  $1/R$ , therefore:

$$I \propto \frac{1}{R} e^{-0.07R} \quad (7.11)$$

where the effect of air absorption has been included. The error in peak location as a function of R is given by Eq. 7.11 and Eq. 7.8 as:

$$\sigma^2(2\theta_p) \propto \frac{R}{T \exp[-0.07R]} \quad (7.12)$$

As R increases the error in peak location increases if T is kept constant.

If it is assumed that each peak is determined to the same precision, the error in stress for the two tilt technique can be written as

$$\sigma(\sigma_\phi) \propto [\sigma^2(2\theta_p)]^{\frac{1}{2}} \quad (7.13)$$

or

$$\sigma(\sigma_\phi) = Q_3 \left[ \frac{R}{T \exp[-0.07R]} \right]^{\frac{1}{2}} \quad (7.14)$$

where Eq. 7.12 has been substituted into Eq. 7.13. The proportionality

constant  $Q_3$  depends on all the proportionality factors in Eq. 7.6 through Eq. 7.13 and must be experimentally determined for each sample. Consequently,  $Q_3$  was determined from data for the position sensitive detector for three samples measured using the two tilt technique.

These three samples cover the range of peak breadths and  $Q_3$  is tabulated in Table 7.1

### 7.3.2 Relations Between Systematic Errors and the Sample-to-Detector Distance

In any residual stress measurement utilizing X-ray diffraction systematic errors arise due to misalignment of the equipment. The most important errors are sample displacement and  $\psi$ -axis missetting which are both dependent on  $R$ . Another error inherent with the PSD arises due to calibration of the detector. The PSD is calibrated at a specific sample to detector distance so that slight displacements of the sample will cause the calibration constant to be slightly incorrect. The formulae for each systematic error is derived assuming the two tilt method is to be used with a stress constant,  $K$ , of  $600 \text{ MPa}^{(100)}$  ( $87020 \text{ psi}$ ) for a  $\psi$  tilt of  $45^\circ$ .

#### (A) Error due to Sample Displacement

Denoting the error in the sample to detector distance as  $\Delta X$ . For the two tilt method, using  $\psi=45^\circ$  and  $\theta=78^\circ$  (a typical value for steel using the  $\text{CrK}\alpha$  211 peak) the error can be simplified to:

$$\sigma_{SD}(\sigma_\psi) = -K \cdot \Delta X \cdot \frac{360}{\pi} \frac{\cos\theta}{R} \left[ 1 - \frac{\sin\theta}{\sin(\theta+\psi)} \right] = Q_4 \cdot \Delta X/R \quad (7.15)$$

TABLE 7.1  
PROPORTIONALITY FACTOR  $Q_3$  FOR THREE STEEL SAMPLES  
( $R=14.55\text{cm}$ )

Sample	Breadth ( $^{\circ}20$ )	Time (sec)	Stress* MPa (psi)	Error* MPa (psi)	$Q_3$ $\text{MPa} \cdot \text{sec}^{\frac{1}{2}}$
1090-1	.45	100	31.4 (4550)	$\pm 4.5$ ( $\pm 650$ )	7.09
1045-3	3.4	200	-718.4 (-104200)	$\pm 6.87$ ( $\pm 1070$ )	16.44
1045-2	6.0	200	-412.3 (-59,800)	$\pm 9.69$ ( $\pm 1469$ )	21.66

\*Obtained from Table 3.12.

where  $Q_4 = 2377$  MPa for the typical values given above.

(B)  $\psi$ -Axis Missetting

For a portable device the detector and X-ray tube must be inclined to accomplish the  $\psi$  tilt. Inherent in the design of the device, the  $\psi$ -axis or pivot point of the instrument must coincide with the  $2\theta$  axis; that is, the primary beam must intersect the axis of rotation. If the construction of the device is accurate enough the X-ray tube and detector will always pivot about the  $\psi$ -axis and there will be no  $\psi$ -axis missetting.

(C) Calibration Constant

The calibration constant in converting position along the PSD into degrees  $2\theta$  is dependent on the sample-to-detector distance. This error can be derived as follows. The angular range covered by the PSD is given by:

$$2\theta = \frac{180}{\pi} \tan^{-1} (D/R) \quad (7.16)$$

where  $D$  represents the length of the detector slit. This is the angular range in degrees covered by the detector at a distance  $R$  from the sample. The calibration constant depends on the number of channels in the MCA in which the data across the length of the PSD is stored. Setting this number to 512, a typical storage division used in the MCA, the calibration constant can be written as:

$$K(R) = \frac{2\theta}{512} = .112 \tan^{-1} (D/R) = \text{degrees per channel} \quad (7.17)$$

The quantity  $K(R)$  is determined for a fixed  $R$  using a calibration sample.

If the specimen being analyzed is displaced by  $\Delta X$ , the calculated peak shift will be in error because  $K(R)$  will be slightly incorrect. For the two tilt method using a stress constant of  $600 \text{ MPa}/^{\circ}2\theta$  the calibration constant error,  $\sigma_{cc}(\sigma_{\varphi})$ , can be written as:

$$\sigma_{cc}(\sigma_{\varphi}) = 600 * \Delta N [K(R) - K(R+\Delta X)] \quad (7.18)$$

where  $\Delta N$  represents the peak shift in channels in the PSD due to the stress in the sample. In terms of  $^{\circ}2\theta$ ,  $\Delta N = \Delta 2\theta/K(R)$  so eq. 7.18 becomes:

$$\sigma_{cc}(\sigma_{\varphi}) = 600 * \Delta 2\theta \left[ \frac{K(R) - K(R+\Delta X)}{K(R)} \right] \quad (7.19)$$

For a  $1^{\circ}$  peak shift and a sample displacement of .5mm, this error is only 2 MPa (290 psi) for a value of  $R = 14.55\text{cm}$  and  $D = 10\text{cm}$ .

The systematic errors that are a function of  $R$  must be combined. It was shown that the psi axis missetting error could be eliminated in construction and that the calibration error was very small, therefore only the sample displacement error need be considered in determining the optimum sample-to-detector distance.

### 7.3.3 Calculation of Optimum Sample to Detector Distance

The factors influencing the accuracy of the residual stress measurement which are a function of  $R$  have been derived. These include the counting statistical error, given by Eq. 7.14, and the sample displacement, given by Eq. 7.15. The sample displacement error  $\Delta X$  in Eq. 7.15, is a nonrandom error, actually a correctable bias in each measurement if it is

measured. If, however, it can be said that on the average the apparatus is positioned within  $\pm \Delta X$  of the correct position, this error can be treated as a random quantity having a normal distribution and can be combined with the statistical error in the following manner:

$$\sigma(\sigma_\varphi) = \left[ Q_3^2 [R/Te^{-0.07R}] + Q_4^2 \left(\frac{\Delta X}{R}\right)^2 \right]^{\frac{1}{2}} \quad (7.20)$$

where  $\sigma(\sigma_\varphi)$  is the total error in the measurement and  $\Delta X$  and  $R$  are in cm. The value of  $Q_4$  is 2377 MPa for  $\psi=45^\circ$  and  $\theta=78^\circ$ .

The time versus sample-to-detector distance is plotted in Fig. 7.3 and Fig. 7.4 for the 1045-2 sample representing a very broad diffraction profile ( $6^\circ 2\theta$  at half maximum). Fig. 7.3 represents the solution to Eq. 7.19 for one standard error of  $\pm 20$  MPa ( $\pm 2900$  psi). When the sample displacement is zero, the instrumental error is non-existent so the time for a fixed error decreases with  $R$ . For only a .05cm error in positioning, however, the minimum time is 35 sec at  $R=8$ cm. Fig. 7.4 represents the solution for an error of  $\pm 40$  MPa ( $\pm 5800$  psi) and for a positioning error of .05cm the minimum time is quite small, 4 sec with a value of  $R$  of 5cm. For an error of 0.1cm in positioning the optimum sample-to-detector distance is 9cm giving a time of analysis of 10 sec.

From this treatment one can judge how accurately the positioning must be and obtain an estimate of the minimum sample to detector distance for a predetermined accuracy. Even for rapid measurements, positioning errors of 1mm should be possible to obtain on a flat surface so for an error of  $\pm 40$  MPa, the sample-to-detector distance could be as short as 8cm. This analysis is based on the sample having the broadest profile obtained in

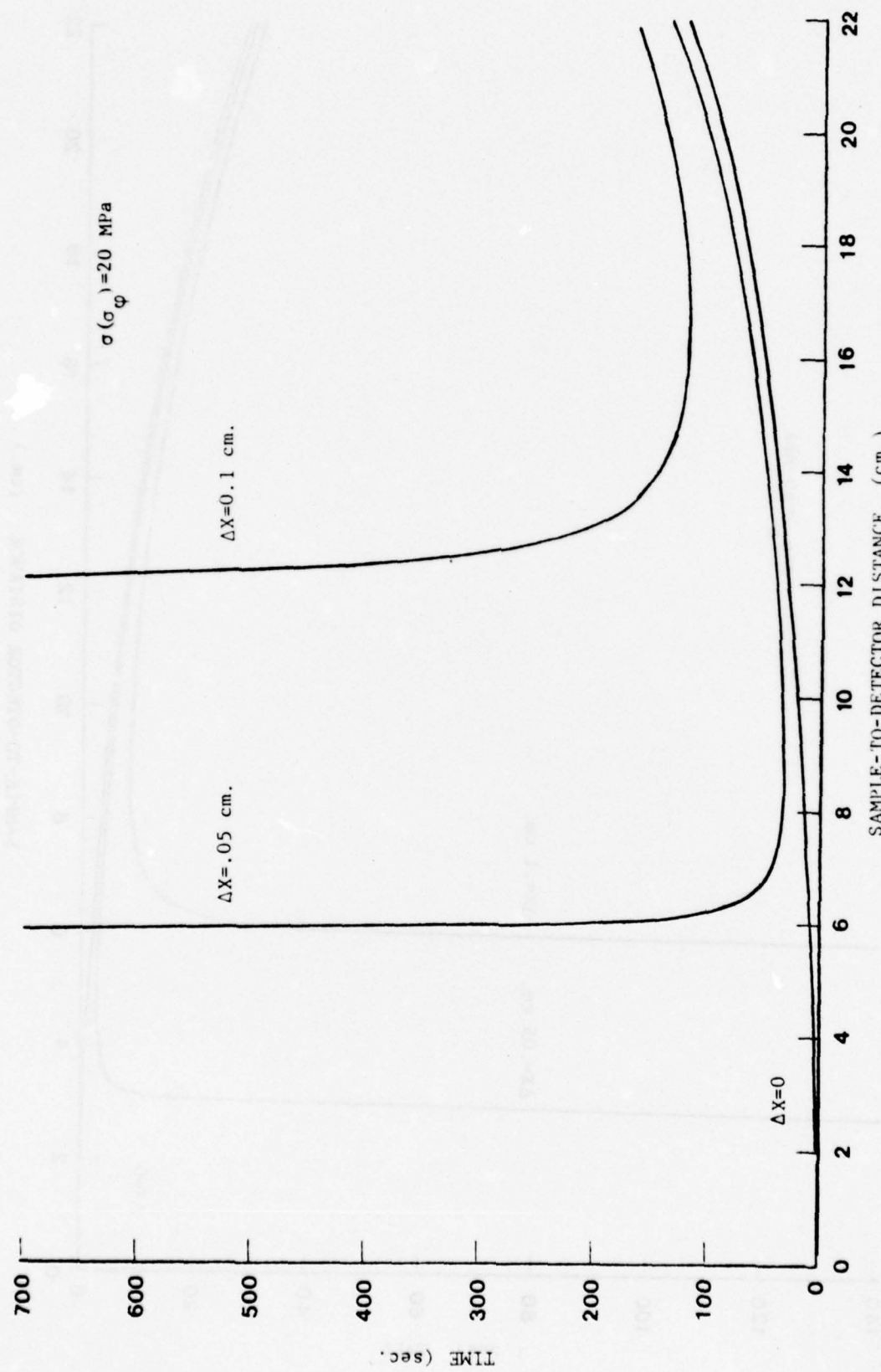


FIGURE 7.3 Optimum sample-to-detector distance for a fixed error of 20 MPa.  
1045-2 sample.

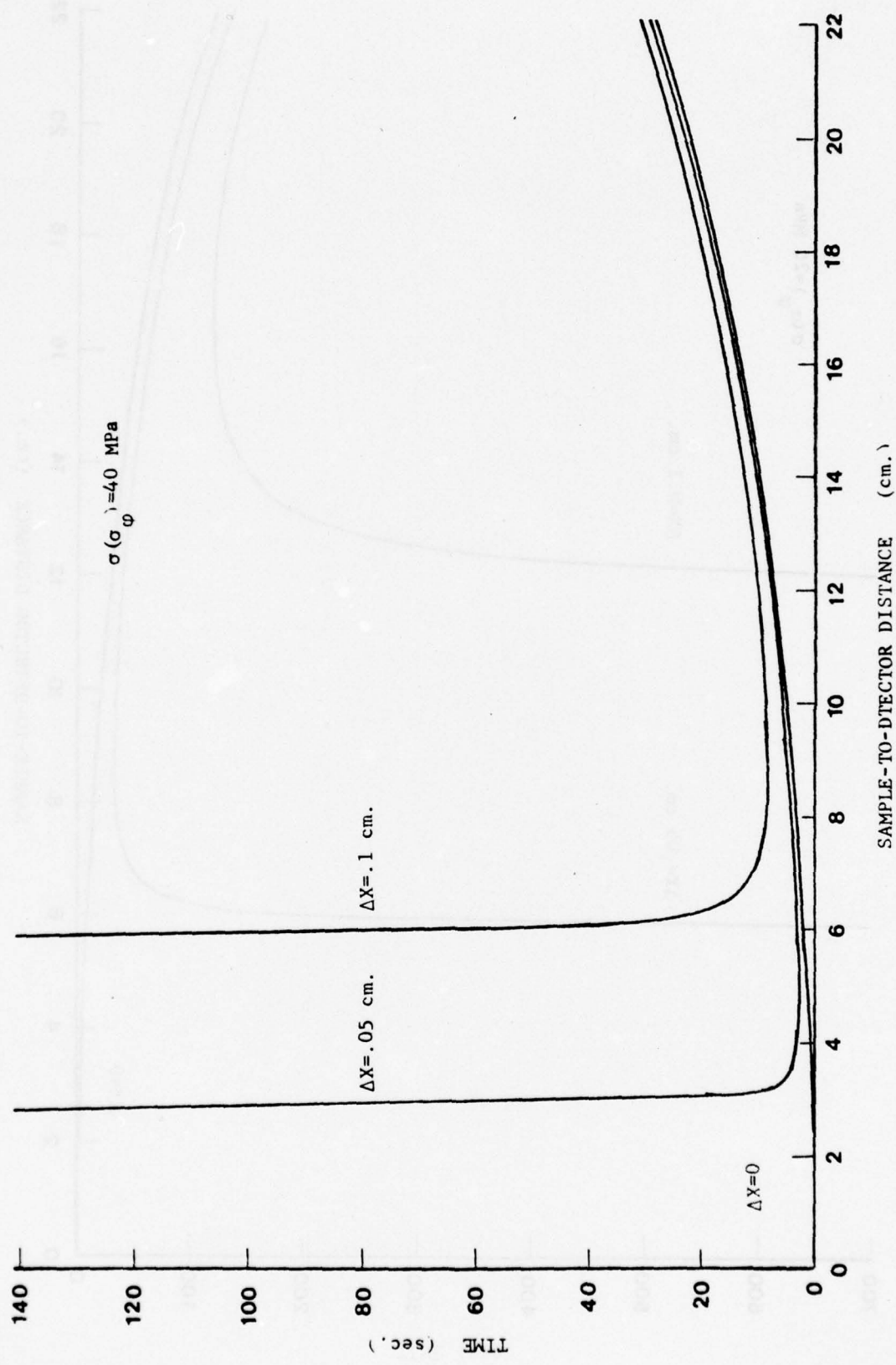


FIGURE 7.4 Optimum sample to detector distance for a fixed error of 40 MPa.  
1045-2 sample

this study. For sharper profiled samples the distance could be shortened. The basic intent of this analysis was to obtain an idea of the best sample-to-detector distance which is shown to be about 8cm, depending on the type of samples and the precision of the measurement. However, it is obvious from Fig. 7.3 and Fig. 7.4 that sample displacement errors play a larger role than absorption of the X-ray beam in air because at short R distances, the displacement prohibits the measurement to the desired accuracy while if the distance were increased to twice the optimum, say 16cm, the counting times are not significantly different.

#### 7.4 DESIGN OF A PORTABLE X-RAY STRESS ANALYSIS SYSTEM

A design for a rapid and portable X-ray stress analyzer using the two tilt method is presented. The two tilt method has been shown to be as accurate as the  $\sin^2\psi$  method when a PSD is used for data accumulation provided  $d$  vs  $\sin^2\psi$  is linear.

##### 7.4.1 Components

A 50kV - 2mA miniature X-ray tube and solid state power supply was borrowed from Watkins-Johnson Co., Palo Alto, California. The X-ray tube, schematically depicted in Fig. 7.5 weighs only 2.3 kg and is air cooled enhancing the tubes use on a portable device. The X-ray tube, described in ref. 108, utilizes a non-intercepting grid electron gun to focus the electron beam so that less power is necessary (and less heat generated) to produce an equivalent X-ray flux as in a conventional sealed X-ray tube. The X-ray tube uses a spot focus and the target is mounted such that the target normal is  $24^\circ$  from the electron beam giving a take-off angle of  $24^\circ$ . Using the 1045-3 specimen and similar sample-to-detector distances, the integrated intensity across the PSD was compared using a Picker Cr X-ray tube (50kv-11mA) and the miniature Cr X-ray tube (50kv-2mA). The diffracted

\* The target is tilted about an axis parallel to the diffraction plane, rather than around an axis perpendicular to this plane, as in a normal tube.

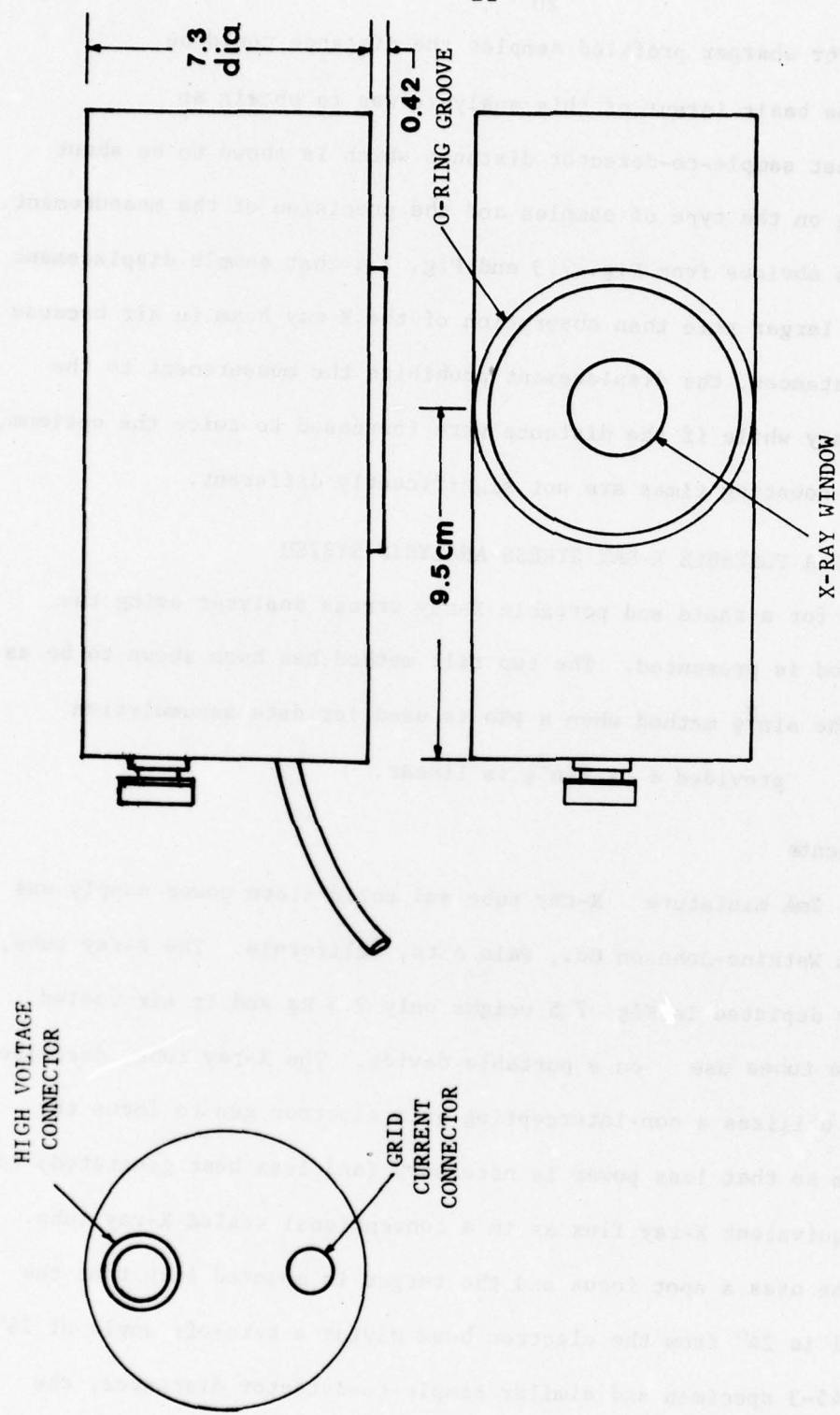


FIGURE 7.5 Outline drawing of the air-cooled X-ray tube.

intensity from the miniature tube was 1.2 times greater for the Picker X-ray tube.

To make the design more compact, a new packaging arrangement for the PSD was borrowed from Tennelec Inc., Oak Ridge, Tennessee. The detector was 20x13x4.5cm with an active length of 10cm used to detect photons. The detector electronics are identical to those described in ONR TR No. 11. The computer program, STRSPD, described in ONR TR No. 16 was used to transfer data from the MCA to the computer and to calculate the stress.

#### 7.4.2 Design

The relationship between the sample-to-detector distance,  $R$ , and the time of analysis was shown in Sec 7.3 not to be critical except at small values of  $R$ . The distance, therefore, must be regulated by the size of the components such as the X-ray tube and detector.

As shown in Fig. 7.6 the size of the X-ray tube dictates the minimum sample-to-detector distance necessary to obtain a back reflection diffraction angle of  $160^{\circ}2\theta$ , in the vicinity of the usual angle for stress measurements. The PSD must be located directly behind the X-ray tube as shown in Fig. 7.6 so that large  $2\theta$  angles can be reached. The sample-to-detector distance is the sum of the minimum distance,  $R_1$  in Fig. 7.6, that can be used to obtain the high angle and the distance,  $R_2$ , that the PSD is located from the point of tangency of the X-ray tube to the beam, point 0. As a result, the sample-to-detector distance is 21cm in this mock-up.

The need to measure the residual stresses on bulk samples requires the  $\psi$  tilt to be made by rotating the instrument instead of the usual practice of inclining the specimen. To accomplish this, the X-ray tube and detector were mounted on a dovetail track allowing a motion of

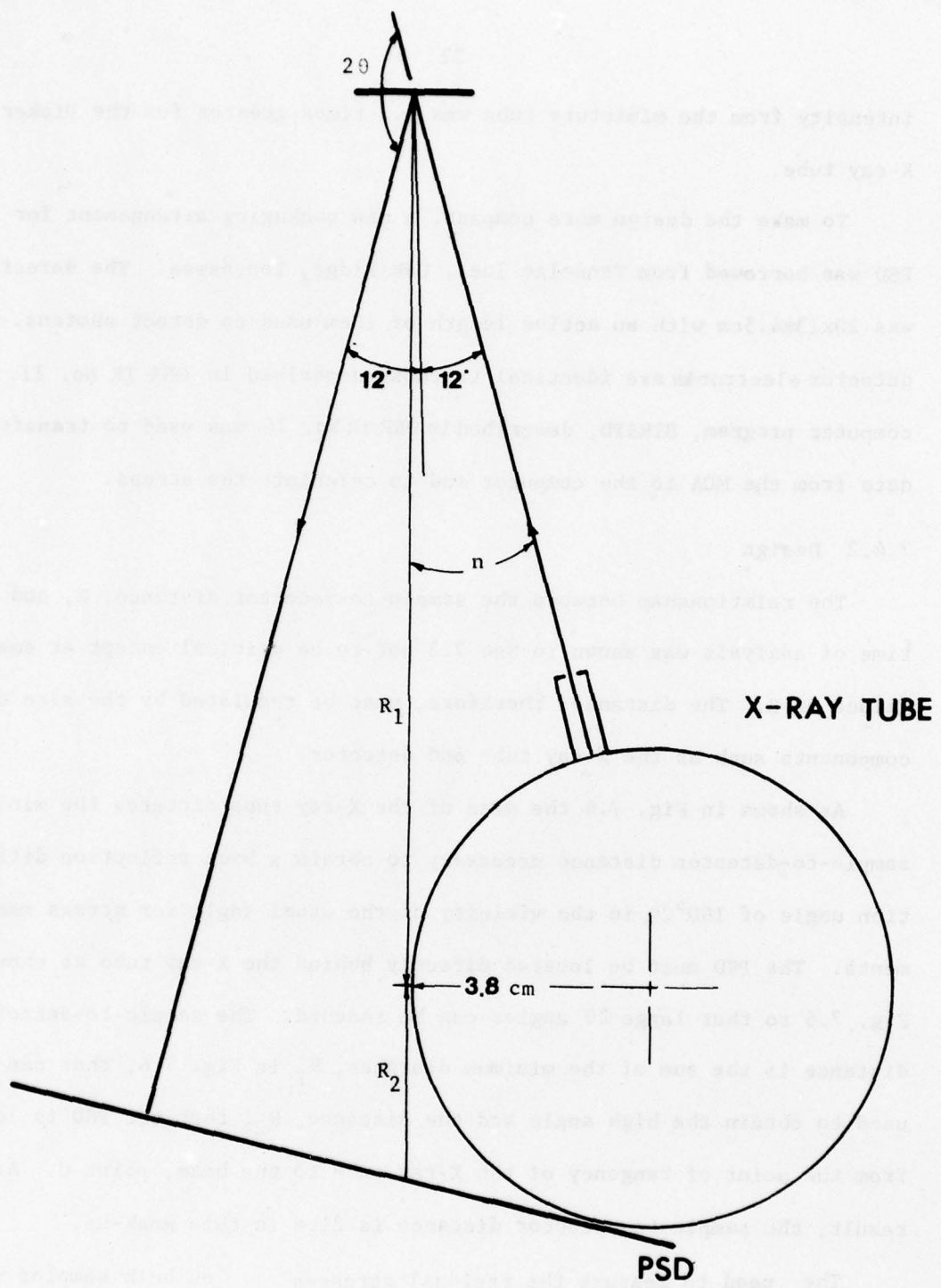


FIGURE 7.6 Schematic drawing showing the minimum sample to detector distance for the air-cooled X-ray tube. This distance is determined by the maximum diffraction angle necessary.

45°. Fig. 7.7 depicts the dovetail track with the X-ray tube and detector mounted. A .8cm thick plexiglass shield was included as a safety precaution to absorb fluorescent radiation.

Positioning of the device was accomplished using a three point bumper system. As seen in Fig. 7.8, the three fingers were mounted so that at  $\psi = 0$  the primary beam was 12° off the normal to a flat sample surface at  $\psi = 0$  constituting an expected diffraction angle of  $156^{\circ}2\theta$ , a typical value for Fe but also suitable for Al because a range of 10° can be seen in the detector. The X-ray tube was positioned so the primary beam intersects the sample at the center of rotation, 0.

Supports for mounting and carrying the device are shown in Fig. 7.9 and Fig. 7.10. Fig. 7.9 shows the detector being used on its stand at  $\psi = 45^{\circ}$ . The entire head assembly weighed 11 kg and could be supported by one person as shown in Fig. 7.10.

Fig. 7.11 shows the diffraction profile from two samples as it appeared on the MCA cathode ray screen. The 1090-1 sample having a sharp profile is shown in Fig. 7.11a. The background on the high angle side of the peak is blocked by the X-ray tube but since only the intensity within the top 15% of the profile is used no error is introduced. The same effect is seen in Fig. 7.11b for the 1045-2 having a broad profile.

#### 7.5 EXPERIMENTAL TESTS

The portable residual stress device was designed to work on large flat surfaces. In order to determine the accuracy of the device, four steel samples previously measured on the diffractometer were analyzed. The samples were mounted on a large steel plate with the surface of each

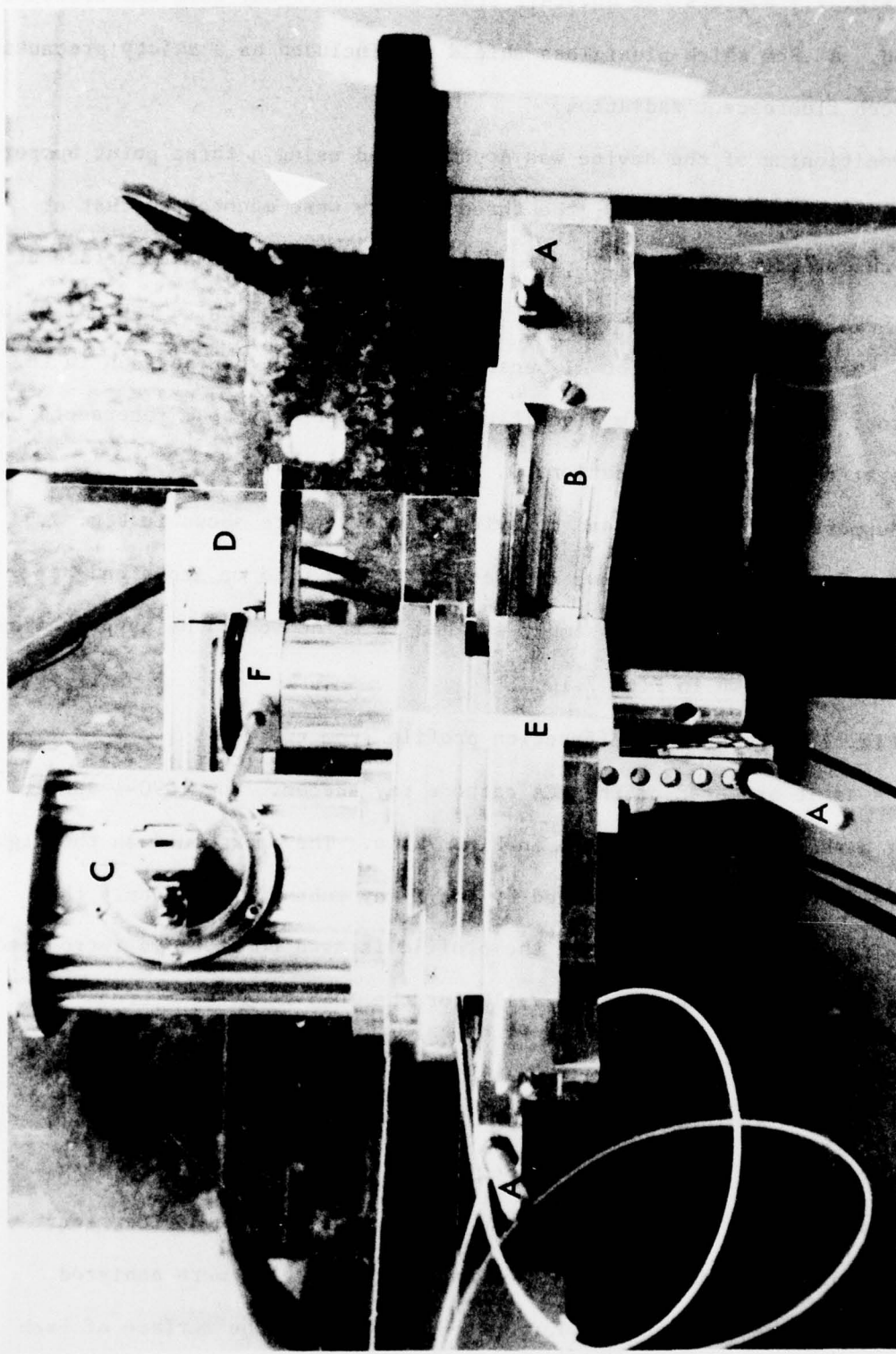


FIGURE 7.7 Front view of the portable residual stress analyzer. The positioning bumpers (A) are located on the stationary or female member of the circular dovetail bracket (B). The X-ray tube (C) and detector (D) are mounted on the left side. The moveable dovetail bracket (E). A distance indicator (F) is used to set the correct sample-to-detector distance when using small samples.

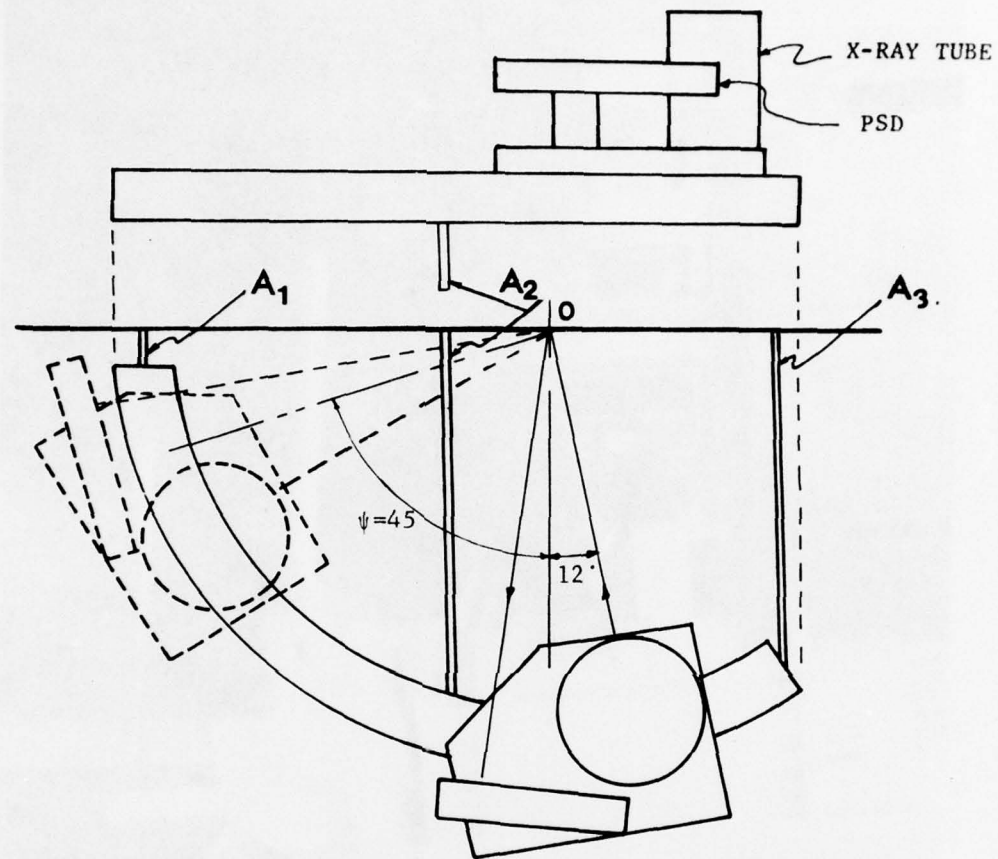


FIGURE 7.8 Schematic drawing depicting movement of the head during a  $45^\circ$  tilt.  $A_1$  represents the positioning bumpers with  $A_1$  and  $A_3$  lying on a horizontal plane and  $A_2$  below this plane fixing the primary beam perpendicular to the sample surface.



FIGURE 7.9 Portable residual stress analyzer located at  $\psi=45^\circ$ . The three bumpers ( $A_1, A_2, A_3$ ) position the apparatus on the flat plate (B). The device can be manually held using the saw handle (C) for support or mounted on the stand (D) and rolled into position.

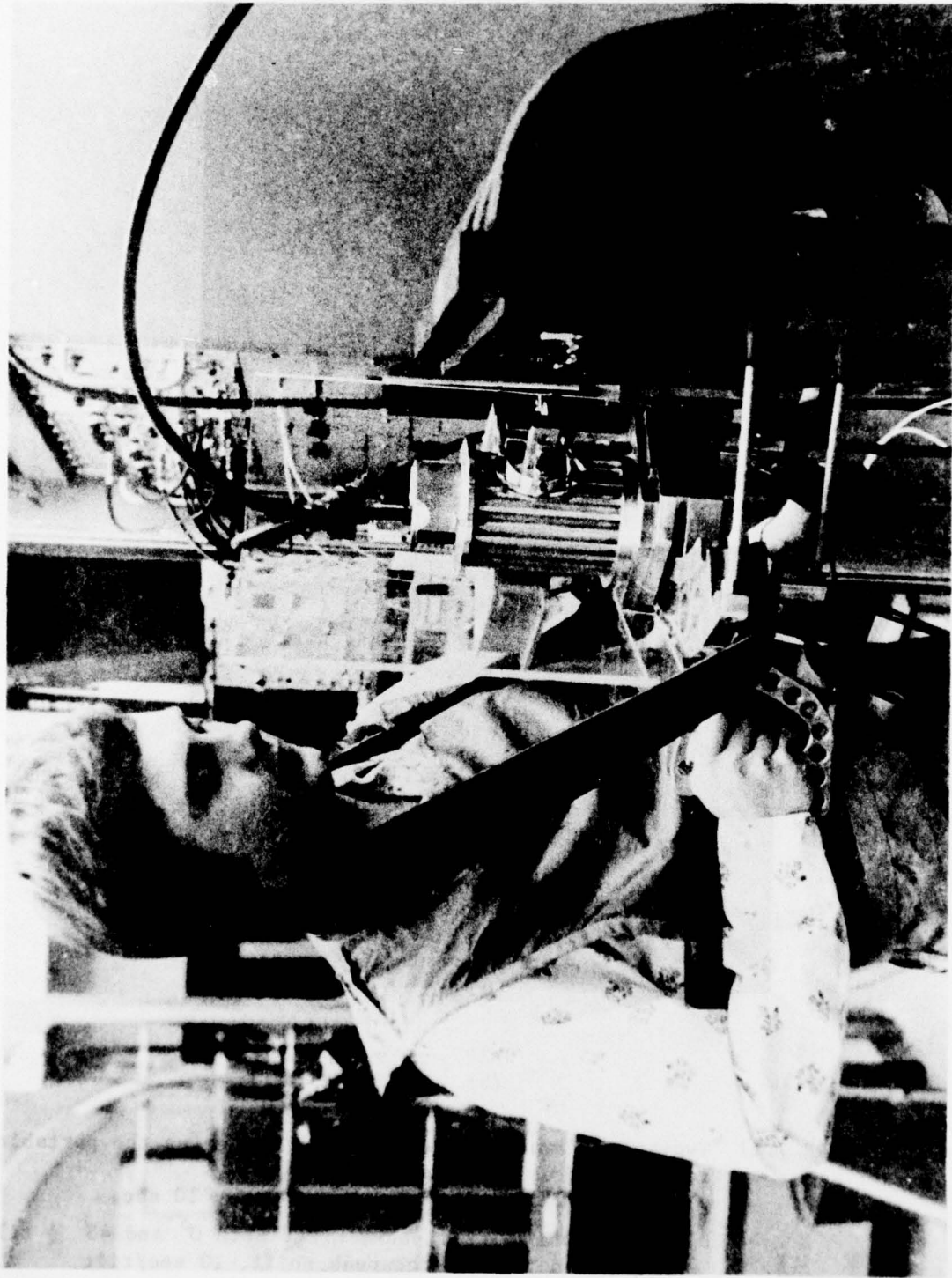
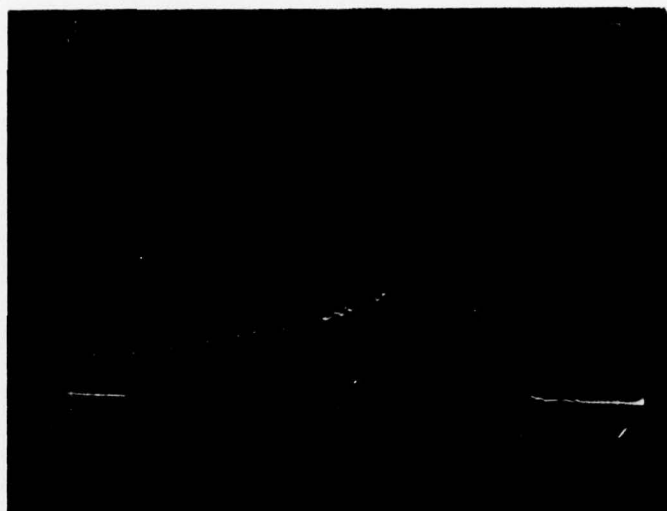
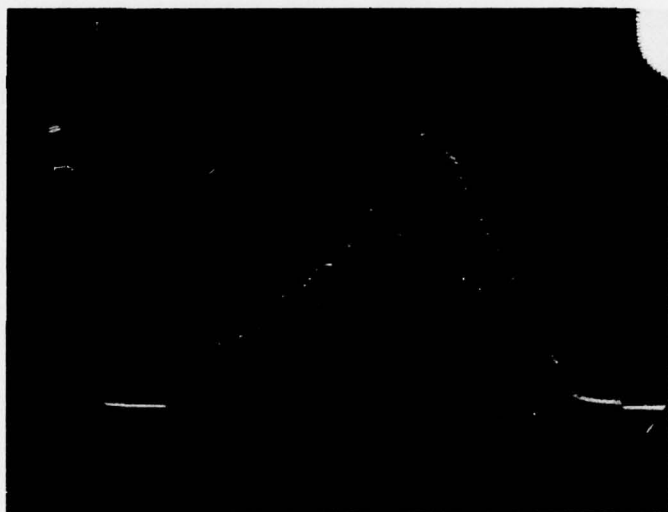


FIGURE 7.10 Manual measurement of residual stress. The neck strap and right hand of the operator support the apparatus while the left hand is used to tilt the X-ray tube and detector with a second handle.



2 $\theta$  →  
(a)



2 $\theta$  →  
(b)

FIGURE 7.11 Typical diffraction pattern obtained using the portable residual stress analyzer.  
a) 1090-1 sample,  $\psi=0^\circ$ , 211 peak, CrK $\alpha$ , 10 sec.  
b) 1045-2 sample, 211 peak, CrK $\alpha$ . Both  $0^\circ$  and  $45^\circ$   $\psi$  tilts are given to show the peak shift, 10 sec/tilt.

sample being flush with the surface of the plate, as seen in Fig. 7.10. This was accomplished by milling a recess equal to the thickness of each sample into the plate. The portable device could then be butted up to the plate and each sample measured.

The results for the four samples are given in Table 7.2. Column 2 tabulates the total time of the measurement for each sample. Column 3 tabulates the average stress found on each sample using the diffractometer.

Column 4 gives the average stress over five measurements using the portable analyzer with the observed error of one standard deviation tabulated in Column 5 and the average counting statistical error in Column 6.

In all cases, the stress was within two standard errors (as given by the counting statistics) of the value measured on the diffractometer, with the average value being quite close. The time of analysis indicates the device is capable of very rapid measurements. A total measurement time of 20 seconds (for both tilts) gives acceptable errors of  $\pm 36.7$  MPa ( $\pm 5315$  psi) on the broadest profiled sample. As seen in Fig. 7.4, for a sample-to-detector distance of 21cm, the counting time is 24 sec for an error of  $\pm 40$  MPa ( $\pm 5800$  psi), quite close to the time above.

A crude test of Eq. 7.2. was made using the portable residual stress unit. The X-ray tube and PSD were mounted on a dovetail track which moved perpendicular to the specimen. The sample-to-detector distance could be varied in this manner by 5cm. Since the pivot axis of the dovetail track (the  $\psi$  axis) remained fixed, this motion did not introduce any  $\psi$ -axis missetting or sample displacement. These large movements did require the detector to be recalibrated, however.

---

\* For the 1090-1 sample having a sharp profile a total measurement time of four seconds gave a statistical counting error of  $\pm 34$  MPa.

TABLE 7.2

**REPLICATE MEASUREMENT USING PORTABLE RESIDUAL STRESS ANALYZER**  
 (5 measurements)

Sample	Time (sec)	$\sigma_{\text{p}}^*$ Diffractometer MPa (psi)	$\langle \sigma_{\text{p}} \rangle$ MPa (psi)	Observed error 5 tests MPa (psi)	Statistical error 5 tests MPa (psi)
1090-1	10	+31.6 (+4580)	-11.6 (-1682)	$\pm 25.4$ ( $\pm 3684$ )	$\pm 19.5$ ( $\pm 2828$ )
1045-3	20	-699.2 (-101410)	-703.4 (-102016)	$\pm 28.3$ ( $\pm 4100$ )	$\pm 29.4$ ( $\pm 4264$ )
1045-2	20	-397.1 (-57596)	-396.4 (-57491)	$\pm 42.7$ ( $\pm 6193$ )	$\pm 36.7$ ( $\pm 5315$ )

\*Average value of stress obtained using a normal diffractometer.  
 From Table 3.8.

When the detector was moved forward by 2.5cm (a sample-to-detector distance of 18.5cm), a total counting time of 16 seconds gave an average error of  $\pm 38.6$  MPa ( $\pm 5600$  psi) over three repeated stress measurements. When displacing the detector away from the sample by 2.5cm (a sample-to-detector distance of 23.5cm), a counting time of 30 seconds gave an average error of  $\pm 41.6$  MPa ( $\pm 5950$  psi). These values compare quite closely with those given by Fig. 7.4. for the proper sample-to-detector distance.

It was also possible to test the sample displacement error. The 1045-2 sample was moved forward by 1mm and 2mm using spacers and three repeated stress measurements made at each sample displacement setting for a total counting time of 40 seconds. The average value of the measured stress was -407.2 MPa (-59060 psi) and -420.8 MPa (-61035 psi) at 1mm and 2mm displacements respectively. From Eq. 3.6 in Chapter 3, the expected error for a 1mm displacement ( $R=21$  cm) is approximately -10 MPa (-1400 psi) using a stress constant of 600 MPa (87020 psi). These values of stress are reasonable compared to Table 7.2 and indicate that small displacements of the sample introduce only minor errors.

In summary, the design presented for a portable residual stress analyzer is capable of complete measurement on any sample in under 20 sec. This could be improved upon by decreasing the size of the X-ray tube so that a shorter sample-to-detector distance could be used. However, measurement times on the order of 20 sec. to a statistical accuracy of  $\pm 40$  MPa or less must be considered adequate for most applications.

To make the apparatus truly an in-field unit, the electronics and computer system must be miniaturized. From discussions with the Chemistry Electronics Shop at Northwestern University, it is felt that all the PSD

electronics and a hardware system for data storage and manipulation could be packaged in a box about 50x50x20cm. This box plus the solid state power supply for the X-ray tube (50x50x15cm) would constitute a fixed cabinet including the tube power supply weighing about 35 kg and a portable head weighing 7 kg. \* Fig. 7.12. shows the size of the cabinet incorporating the miniaturized electronics. The only controls necessary are an 'on-off' switch and a high voltage control for the PSD. A trigger to open the X-ray beam for a preset time could be mounted on the hand-held device.

Pressurization of the PSD without gas flow was tested by mounting a high pressure shut off valve at the inlet and outlet gas connections on the PSD. It was found that this particular detector would not remain pressurized. As soon as the two valves were closed, the detector pressure, measured between the detector and the shut-off valve, began to fall. Extensive tests confirmed that the pressure loss was in the detector and not in the gas line connections. The manufacturer of the detector insists, however, that the instrument can be made to hold pressure for at least 12 hours and hopefully, one lasting two or three days is possible. This would enable an operator to pressurize the detector at the beginning of a day and a gas-flow system would be unnecessary. The instrument would then be fully transportable and the measurement could be made by one person holding the 'head'. It is felt that this type of portable instrument can provide the necessary stimulus to enable the X-ray measurement of residual stress to be widely used in industry both as a laboratory and an in-field tool.

\* Although the prototype weighed 11 kg, such components as the dovetail track and X-ray tube shielding could be severely lightened.

\*\* The original PSD was tested and lost only 5 psi over an 18 hour period.

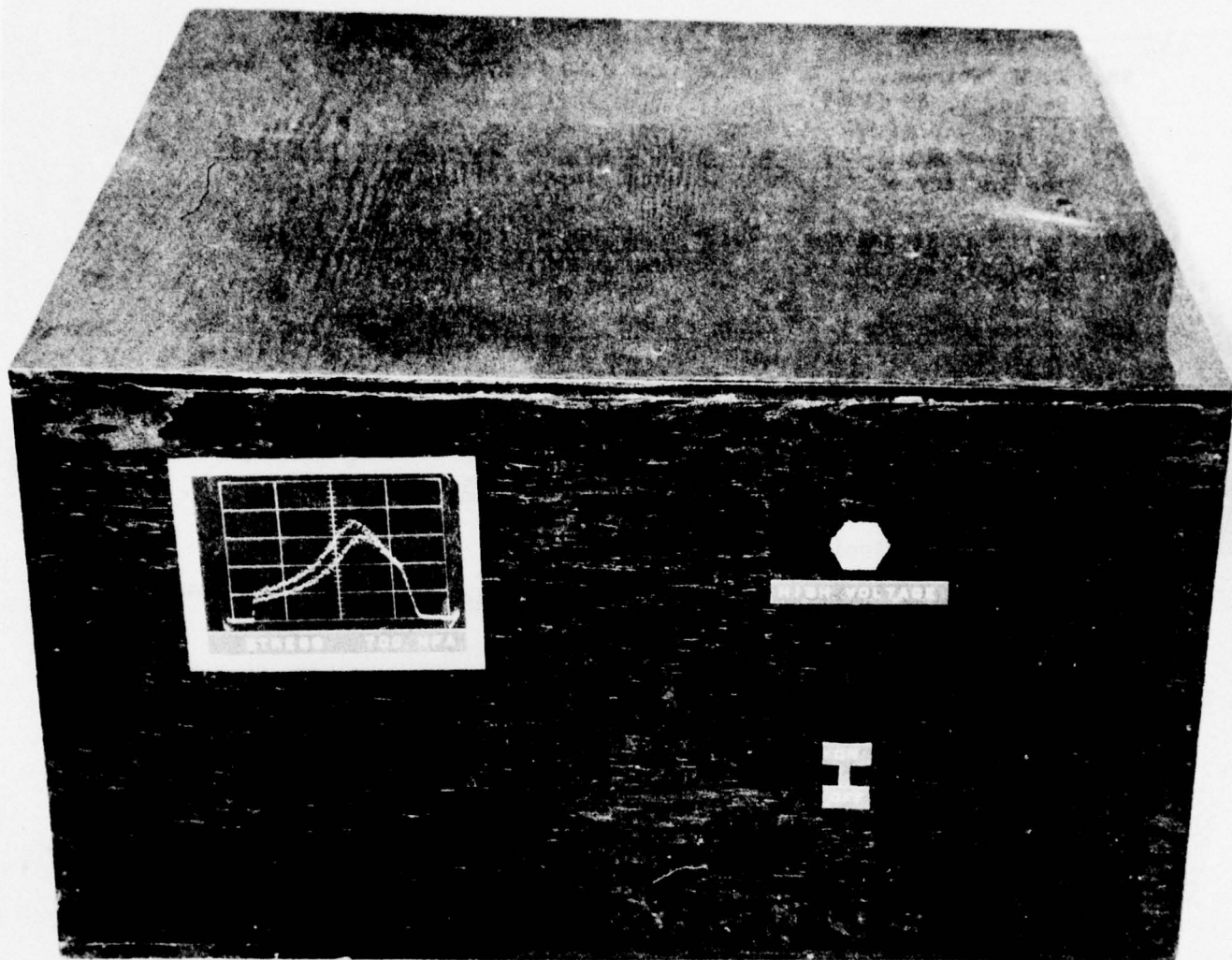


FIGURE 7.12 Proposed cabinet for the miniturized electronics of the portable residual stress analyzer. The only external controls necessary are the 'on-off' switch and a high voltage control. The peak shape and stress would be displayed on a CRT.

## REFERENCES

98. E. W. Weinman, J. E. Hunter, and D. D. McCormack, Metal Progress, 96 No. 1, 88 (1969).
99. K. Kamachi, X-Ray Study on Strength and Deformation of Metals, The Society of Materials Science, Japan (1971), p. 95.
100. Residual Stress Measurement by X-Ray Diffraction- SAE J 784a, 2nd Edition, Society of Automotive Engineers, Inc. (1971).
101. Nondestructive Evaluation of Residual Stress, Proceedings of a Workshop, Air Force Materials Laboratory, NTIAC-76, Southwest Research Institute, San Antonio, Texas (1976) p. 153.
102. United States Patent 3,934,138. (1976).
103. W. C. Giessen and G. C. Gordon, Science, 159, 973 (1968).
104. H. Cole, J. Appl. Cryst. 3, 405, (1970).
105. J. B. Cohen, Diffraction Methods in Materials Science, MacMillan Co., New York (1966) P. 255.
106. International Tables for X-Ray Crystallography, Vol. II, Kynock Press, Birmingham, England (1968).
107. B. E. Warren, X-Ray Diffraction, Addison-Wesley Publ. Co., Reading, MA., (1969).

Unclassified  
Security Classification

DOCUMENT CONTROL DATA - R & D

(Security classification of title, body of abstract and indexing annotation must be entered when the overall report is classified)

1. ORIGINATING ACTIVITY (Corporate author)	2a. REPORT SECURITY CLASSIFICATION Unclassified	
J. B. Cohen, Northwestern University, Evanston, IL	2b. GROUP	
3. REPORT TITLE  A PORTABLE RESIDUAL STRESS ANALYZER		
4. DESCRIPTIVE NOTES (Type of report and inclusive dates) Technical Report No. <b>19</b>		
5. AUTHOR(S) (First name, middle initial, last name) M. R. James and J. B. Cohen		
6. REPORT DATE N00014-75-C-0580	7a. TOTAL NO. OF PAGES 35	7b. NO. OF REFS 10
8a. CONTRACT OR GRANT NO. 5345-455	9a. ORIGINATOR'S REPORT NUMBER(S) Technical Report No. <b>19</b>	
b. PROJECT NO.	9b. OTHER REPORT NO(S) (Any other numbers that may be assigned this report) None	
c.		
d.		
10. DISTRIBUTION STATEMENT  Distribution of this document is unlimited.		
11. SUPPLEMENTARY NOTES	12. SPONSORING MILITARY ACTIVITY Office of Naval Research Metallurgy Branch	
13. ABSTRACT  A portable device for stress measurements based on a position sensitive detector and using a miniature air-cooled X-ray tube was built to demonstrate the potential of such a system. The measuring apparatus, weighing 11 kg, could be held by one person with the electronics housed in a separate cabinet. A variety of steel samples, having from 0 to -700 MPa were tested by comparing measurements made on a diffractometer to those made with the portable device. The device proved to be accurate and accomplished the entire measurement using two $\pm$ tilts to a statistical error of less than $\pm$ 40 MPa in <u>under</u> 20 seconds on all samples. (In some cases in 4 seconds.) The portability of the apparatus and rapid measurement time suggest applications for the X-ray stress measurement never possible before, such as on-sight inspection during fabrication or in-field measurements.		

Unclassified

Security Classification

Information

14. KEY WORDS	LINK A		LINK B		LINK C	
	ROLE	WT	ROLE	WT	ROLE	WT
residual stresses X-ray residual stress measurement portable X-ray unit stress measurement position sensitive detector						